Instructive role of aPKCζ subcellular localization in the assembly of adherens junctions in neural progenitors

Sourav Ghosh*†, Till Marquardt‡§, Joshua P. Thaler‡¶, Nigel Carter*, Shane E. Andrews‡, Samuel L. Pfaff‡‖, and Tony Hunter*‖

*Molecular and Cell Biology Laboratory and ‡Gene Expression Laboratory, Salk Institute for Biological Studies, 10010 North Torrey Pines Road, La Jolla, CA 92037

Edited by Fred H. Gage, Salk Institute for Biological Studies, San Diego, CA, and approved November 12, 2007 (received for review June 18, 2007)

In the neurogenic phase of CNS development, the proliferating progenitors are found medially within the neuroepithelium. The adherens junctions on the apical membrane of proliferating neural progenitors allow for cell–cell adhesion and medial stratification. In contrast, differentiating neuronal precursors delaminate and migrate laterally, establishing the laminar layers. Apical adherens junctions also establish the apical–basal polarity in neural progenitors, which in turn is postulated to lead to asymmetric inheritance of cell fate determinants during neurogenic divisions. The signaling pathways and cellular mechanisms that regulate the assembly and asymmetric localization of adherens junctions in neural progenitors remain elusive. Here we show that atypical PKCζ/λ (aPKCζ/λ) localizes at the apical membrane of proliferating neural stem cells, but not postmitotic neuronal precursors, in the developing chicken neural tube. This precise subcellular compartmentalization of the kinase activity provides an instructive signal for apical assembly of adherens junctions in a PI3K, Rac/Cdc42 signaling-dependent pathway. Apical aPKCζ coordinates neural stem cell proliferation and the overall stratification of cell types within the neural tube.

kinase | signaling | neurodevelopment

Radial glia, the progenitors found in the neurogenic phase, span the neural tube and are characterized by an intrinsic apical (medial)–basal (lateral) polarity (1). Their apical membrane, adjoining the lumen, contains adherens junction proteins and maintains cell–cell adhesion, and the basal process contacts the basement membrane. This polarity is postulated to be involved in establishing the normal structural organization of the pseudostratified neuroepithelium, as well as controlling allocation of cell fate determinants and the specification of daughter cell fate (1). Radial glial cell divisions are of two types: symmetric or proliferative and asymmetric or neurogenic. The former generates two identical daughter cells that remain in the ventricular zone (VZ), whereas asymmetric divisions give rise to a progenitor and a differentiating daughter cell. Both daughters from proliferative divisions inherit adherens junctions and remain in the VZ. In neurogenic divisions, adherens junctions, which are exclusively localized at the apical end facing the lumen, are inherited only by the apical, undifferentiated daughter and maintain that cell in the VZ (1–4). In fact, the apical membrane containing adherens junctions is thought to have determinants associated with it that maintain the neural stem cell fate (1). Correspondingly, cell fate determinants specifying neuronal fate and localized on the basal pole are more likely to be inherited by the basal daughter cell, leading to their differentiation. Therefore, adherens junction localization at the apical membrane in neural progenitors ensures the obligatory and coordinated segregation of these molecules between daughter cells during neurogenic divisions and is an important and defining step in neurogenesis. Coincident with the exit from the cell cycle, differentiating neuronal precursors delaminate from the progenitor layer and migrate along radial fibers into layers concentric with the germinal epithelium to form the mantle zone (MZ). This lateral migration along radial fibers also is contingent on the correct apical–basal polarity in radial glial cells. Hence, the knowledge of molecular mechanisms that regulate apical adherens junctions in these neural progenitors is critical for understanding vertebrate neurodevelopment.

The atypical PKCζ/λ (aPKCζ/λ) is a determinant of cellular and embryonic polarity in *Drosophila* and *Caenorhabditis elegans* (5) and has been implicated in the development of the nervous system. The *Drosophila* ortholog, DaPKC, plays an important role in neuroblast delamination (6, 7). aPKCλ also affects the development of the vertebrate CNS. Neuroectodermal cell adhesion is altered in aPKCλ loss-of-function mutants in *Danio rerio* (8). The conditional KO of aPKCλ in mouse neural progenitors results in the loss of adherens junctions and neuroepithelial tissue architecture (9). Indeed, in cultured epithelial cells, aPKCλ regulates the assembly, but not the maintenance, of adherens junctions (10). The obvious importance of aPKCλ in the assembly of adherens junctions notwithstanding, it remains unknown whether this kinase has an instructive role in the apically restricted assembly of adherens junctions and consequent apical–basal polarity in neural stem cells or whether its requirement is merely permissive. In this regard, the distribution of aPKCζ/λ in the neural tube is interesting. aPKCζ/λ is localized asymmetrically at the luminal margin of the mammalian neuroepithelium (9, 11). The asymmetric division model discussed earlier posits that it is the polarized distribution of aPKCζ/λ in the progenitor radial glia that results in the asymmetric distribution, segregation, and differential inheritance of adherens junctions between neural progenitors and neuronal precursors. However, this hypothetical model has not been tested by using a direct experimental approach. Therefore, through a series of functional analyses in the spinal cord of the chicken embryo, we sought to experimentally test this fundamental assumption that proper localization of adherens junctions, and consequently progenitor polarity and neuronal differentiation, depends on the spatially localized activity of aPKCζ.

Author contributions: S.G., T.M., and J.P.T. designed research; S.G., T.M., J.P.T., and S.E.A. performed research; N.C. contributed new reagents/analytic tools; S.G., S.L.P., and T.H. analyzed data; and S.G. wrote the paper.

The authors declare no conflict of interest.

This article is a PNAS Direct Submission.

†Present address: Basic Medical Sciences, University of Arizona College of Medicine, Phoenix, AZ 85012.

§Present address: European Neuroscience Institute, 37077 Göttingen, Germany.

¶Present address: University of Washington Medical Center, Seattle, WA 98195.

‖To whom correspondence may be addressed. E-mail: pfaff@salk.edu or hunter@salk.edu.

This article contains supporting information online at www.pnas.org/cgi/content/full/0705713105/DC1.

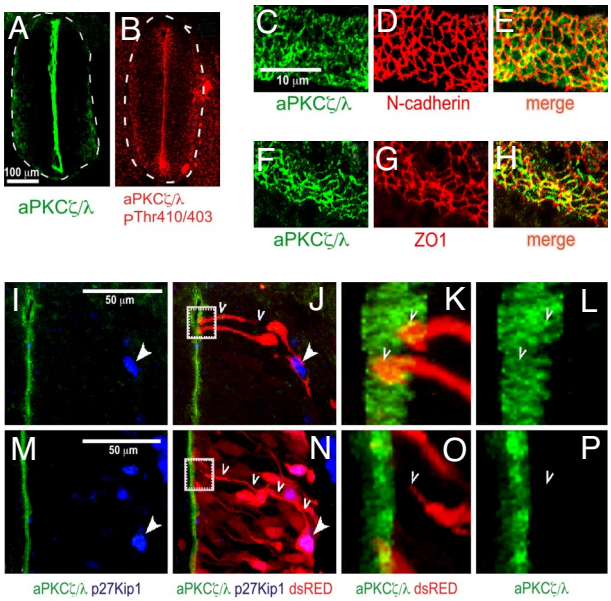

Fig. 1. Localization of aPKCζ/λ in neuroepithelial cells of embryonic chicken spinal cord. (*A* and *B*) Cross-sections through E3 chicken neural tube revealing aPKCζ/λ and active aPKCζ/λ localization at ×10 magnification. (*C–H*) Open-book preparation of E3 neural tube was stained with the indicated antibodies and visualized at ×63 magnification. (*E* and *H*) Merged images show overlapping distribution of aPKCζ/λ and cell-adhesion proteins. (*I–P*) Chicken embryos were microinjected and electroporated at E2 with low amounts of dsRED expression vector to trace the radial processes of individual progenitors in few cells. Embryos were fixed at E3 and E4 and stained with aPKCζ/λ and p27Kip1 antibodies. (*I*, *J*, *M*, and *N*) Twenty optical sections through the *z* axis, 20 nm each, were collected on a Zeiss laser confocal microscope by using a ×63 objective, and this *Z* series was stacked by using PASCAL software. Nuclear-localized p27Kip1 is indicated with solid arrowheads. (*J* and *N*) An individual p27Kip1$^-$ progenitor (*J*) and a p27Kip1$^+$ cell (*N*) are traced with open arrowheads. (*K* and *L*) The area indicated by the dotted box in *J* is magnified to show the end feet of two dsRED-labeled progenitors (open arrowheads). (*O* and *P*) Similar magnification of the area indicated by the dotted box in *N*. The process of the p27Kip1$^+$ cell shown within the boxed area in *N* is magnified in *O* and *P* and traced with open arrowheads. The stacked *Z* series were rotated for the images in *K*, *L*, *O*, and *P*.

Results

aPKCζ/λ Localizes at the Apical Membrane in Proliferating, but Not Postmitotic, Cells. Immunohistochemical analyses using aPKCζ/λ antibodies or activated aPKCζ/λ (phospho-aPKC$\zeta/\lambda^{\mathrm{Thr-410/403}}$) antibodies revealed enrichment at the luminal margin of the neuroepithelium in the chicken embryonic spinal cord (Fig. 1 *A* and *B*). Coimmunofluorescence analyses on open-book preparations of embryonic spinal cords demonstrated that aPKCζ/λ partially overlapped with *N*-cadherin and ZO-1, which are structural components of apical adherens junctions in the neuroepithelium (Fig. 1 *C–H*). Next, we examined the subcellular distribution of aPKCζ/λ within individual neural progenitor cells. Using an *in ovo* microinjection and electroporation technique, we expressed soluble dsRED fluorescent protein in a subset of neuroepithelial cells to visualize the entire apical–basal extent of their radial processes by stacking a confocal series across the neural tube cross-section. These sections were colabeled for aPKCζ/λ and p27Kip1. Expression of the cyclin-dependent kinase inhibitor, p27Kip1, peaks during the beginning of cell-cycle exit in the proliferative neuroepithelium in mouse neocortex (12). The p27Kip1-low/negative, dsRED-labeled progenitors displayed high levels of aPKCζ/λ at the apical margin in every cell examined (n = 35, three different embryos). In contrast, cells showing strong, nuclear p27Kip1 lacked detectable expression of aPKCζ/λ (n = 24, three different embryos) (Fig. 1 *I–P*). These results demonstrate that aPKCζ/λ is apically compartmentalized in proliferating progenitors. Subsequently, as cells exit the cell cycle, delaminate, and migrate laterally, aPKCζ/λ compartmentalization is lost. This differential localization pattern of aPKCζ/λ between neural progenitors and neuronal precursors suggests that the apical compartmentalization of this kinase may regulate the differential stratification of these cell types within the developing neural tube.

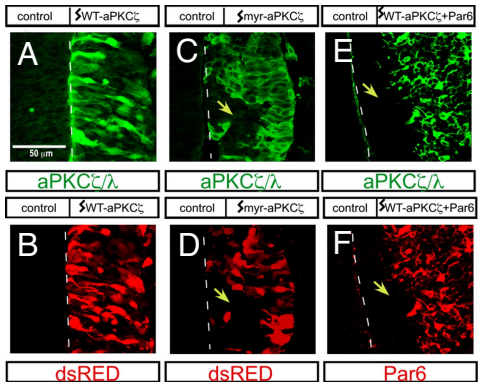

Fig. 2. Disruption of neuroepithelial organization after ectopic plasma membrane localization of aPKCζ. (*A–F*) Neuroepithelial cross-sections from E4 embryos showing aPKCζ/λ (*A*, *C*, and *E*), dsRED (*B* and *D*), and Par6 (*F*) expression. The neural tubes were microinjected and electroporated with WT-aPKCζ or myr-aPKCζ plus dsRED (*A–D*) or WT PKCζ plus Par6 (*E* and *F*) at E2. Disruption in the neuroarchitecture is indicated with yellow arrowheads.

Apical Compartmentalization of aPKCζ Is Essential for Neuroepithelial Architecture. To directly test whether the apical compartmentalization of aPKCζ is essential for proper neural development, we disrupted the endogenous localization by ectopically expressing either WT-aPKCζ or myristoylated aPKCζ (myr-aPKCζ) constructs along with dsRED in the embryonic chicken spinal cord at embryonic day 2 (E2), at which time the neural tube is almost exclusively composed of neural stem cells. At E3, we analyzed transverse sections of spinal cord at thoracic levels for WT-aPKCζ and myr-aPKCζ expression. Both WT-aPKCζ and myr-aPKCζ were detected throughout radial glial cells, but myr-aPKCζ was localized to the membrane because myristoylation targets aPKCζ to the plasma membrane along the entire apical–basal axis of cells (i.e., not spatially restricted), whereas exogenously expressed WT-aPKCζ was diffuse and cytoplasmic (Fig. 2 *A* and *C*). Neither WT-aPKCζ alone (Fig. 2 *A* and *B*) nor dsRED alone (data not shown) disrupted the neuroepithelial architecture because the electroporated progenitors spanned normally from the apical lumen to the basal surface of the neural tube. In contrast, the expression of myr-aPKCζ led to a marked disruption of radial glial organization. Often the apical attachments were lost, and cells failed to contact the lumen and showed abnormal delamination away from the midline (indicated by dotted line) in many areas (yellow arrows indicate sites where cells were displaced away from the midline) (Fig. 2 *C* and *D*).

aPKCζ and the partition-defective (Par) scaffold proteins such as Par6 interact directly with each other to form a functional complex (13). We tested whether the effects of myr-aPKCζ could be recapitulated by coexpressing WT-aPKCζ together with Par6A. Indeed, the coexpression of Par6A resulted in plasma membrane localization of WT-aPKCζ throughout the apical–basal axis of the cells (Fig. 2*E*) and phenocopied myr-aPKCζ-induced disruption of the neuroepithelium (yellow arrows indicate areas in which cells were displaced away from the lumen marked with a dotted line) [Fig. 2 *E* and *F*, Table 1, and

Table 1. aPKCζ-Par6 is regulated by signals from PI3K and Rac/Cdc42 pathways

Constructs	Progenitors outside VZ, %
myr-aPKCζ	64 ± 12
WT-aPKCζ	0
aPKCζK281W	0
myr-aPKCζD62,66A	60 ± 15
myr-aPKCζK281W	0
aPKCζA119D	15 ± 10
myr-aPKCζC-term(246–623)	21 ± 9
myr-aPKCε	0
Par6	0
Par6 + WT-aPKCζ	57 ± 18
Par6 + WT-aPKCζK281W	0
Par6 + WT-aPKCζD62,66A	0
Par6ΔCRIB	0
Par6ΔCRIB + WT-aPKCζ	0
Par6 + aPKCζT410A	0
GSK3βWT	0
GSK3βS9A	0
myr-aPKCζ+GSK3βWT	18 ± 11
myr-aPKCζ+GSK3βS9A	11 ± 7

The indicated aPKCζ, Par6, and GSK3β expression constructs were microinjected and electroporated into the chicken neural tube at E2, and progenitor cell-stratification defects were assayed by the extent of aberrant delamination of $Pax7^+$ cells at E4. The severity of the delamination phenotype is represented as a percentage of $Pax7^+$-regionalized progenitors present outside the VZ.

supporting information (SI) Fig. 5*E*]. In control experiments, Par6A alone did not disrupt the neuroepithelial cytoarchitecture (see Table 1 and SI Fig. 5*D*). The unrestricted plasma membrane distribution of aPKCζ, after myristoylation or coexpression with Par6A, effectively overrides the normal subcellular compartmentalization of endogenous aPKCζ/λ and disrupts neuroepithelial tissue organization.

Mislocalization of aPKCζ Results in the Aberrant Distribution of Cell Adhesion Molecules and Disrupts Apical Adherens Junctions and Neural Progenitor Polarity. How does the mislocalization of aPKCζ activity result in the delamination of neural progenitors? Adherens junctions are critical for radial glial polarity and neuroepithelial cytoarchitecture (1). This finding prompted us to test whether the aberrant localization of myr-aPKCζ affected the assembly and/or maintenance of apical adherens junction proteins within neural progenitors. Immunohistochemical analyses 12 h after electroporation show that ZO-1 is localized at the midline in the neural tube (Fig. 3*A*) and apically within neuroepithelial cells (Fig. 3*A Inset*). Expression of myr-aPKCζ resulted in aggregates of ZO-1 away from the midline in the neural tube (marked by yellow arrowhead in Fig. 3*C*) and away from the apical membrane within individual basally displaced myr-aPKCζ-expressing cells (Fig. 3*C Inset*, yellow arrowheads). By 36 h after electroporation, adherens junction proteins were detected in a disorganized pattern overlapping that of myr-aPKCζ in the MZ area of the tissue (Fig. 3 *E–G*, yellow arrowheads). Correspondingly, staining was absent at the normal localization sites at the midline (Fig. 3 *E–G*, white arrowheads). In contrast, when WT-aPKCζ was expressed, the distribution of adherens junction proteins was not unlike that on the control unelectroporated side (SI Fig. 5 *H–K*). Thus, the normal, polarized, subcellular compartmentalization of adherens junction proteins within cells is lost when myr-aPKCζ is expressed, and these cells are abnormally displaced away from the midline within the neural tube. Loss of proper localization of adherens junction proteins within cells may lead to a loss of apical–basal

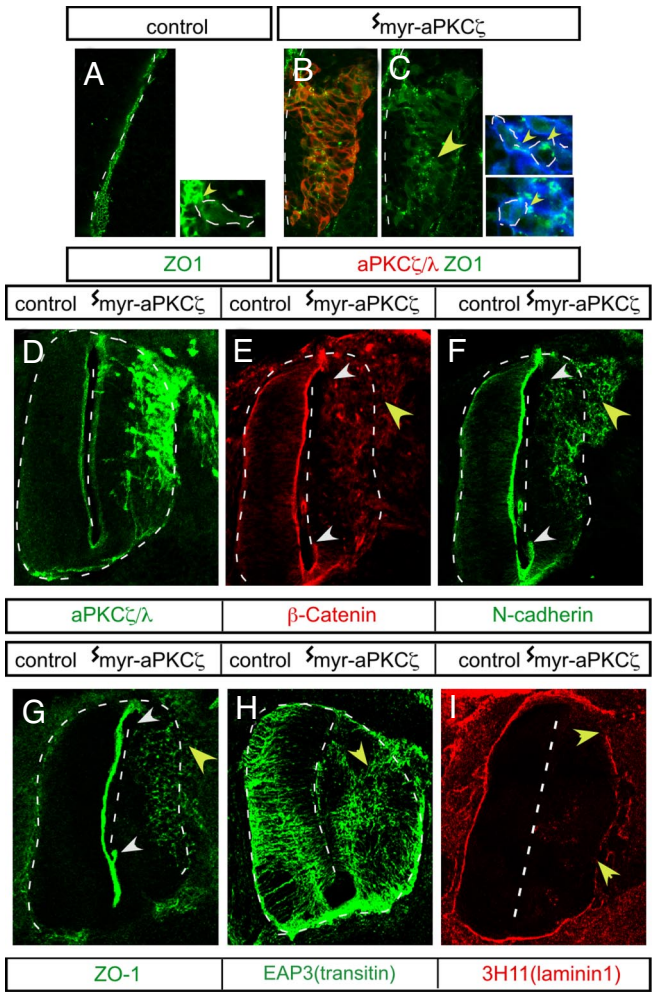

Fig. 3. Redistribution and loss of apical adherens junction proteins and disruption of basal lamina after myr-aPKCζ expression. (*A*) Normal apical localization of ZO-1 at the apical, luminal margin. (*B–I*) Ectopic localization of adherens junction proteins at E3 (*B* and *C*) and E4 (*E–G*) or disruption of apical–basal polarity in radial glial processes at E4 (EAP3 antitransitin intermediate filament antibody staining) (*H*) and basal lamina at E4 (chicken laminin 1 antibody staining) (*I*) after introduction of myr-aPKCζ (*B–I*) at E2. Abnormal distribution is indicated with yellow arrowheads. (*E–G*) The region of the midline showing loss of apical junction proteins is indicated within white arrowheads.

polarity. Indeed, after expression of myr-aPKCζ, immunohistochemical analyses with EAP3 antibodies that stain the intermediate filament protein transitin in radial glia (14) indicated that cells lost the normal apical–basal orientation of their processes (Fig. 3*H*). The basal lamina of the neural tube was disrupted, and some laminin1 staining was observed within the neural tube (Fig. 3*I*). Abnormally delaminating cells were observed to stream out of the neural tube at sites where the basal lamina was not intact. Occasionally, ectopic neuroblastic rosette-like structures were observed in the neural tube (SI Fig. 5 *L–P*). Interfering with structural adherens junction proteins in the chicken tectum was previously reported to have similar effects (15). Furthermore, some Numb crescents, which are cell fate determinants basally localized in mitotic neuroepithelial cells (16), were mislocalized (SI Fig. 5 *Q–U*), confirming that the normal apical–basal polarity is disrupted after the expression of myr-aPKCζ. Thus, it is likely that the spatially localized apical aPKCζ activity has an instructive role in the consonant localization for adherens junction proteins and apical–basal polarity in neural progenitors. Loss of

NEUROSCIENCE

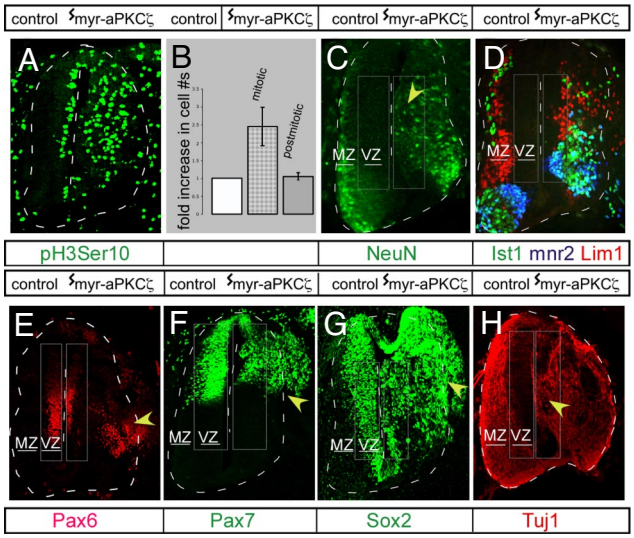

Fig. 4. Disruption of progenitor number, localization, and medial-lateral stratification of neural layers after expression of myr-aPKCζ. (*A–C*) Displacement of mitotic (ph3Ser10 staining) (*A*) and NeuN$^+$ nuclei after expression of myr-aPKCζ (*C*) (indicated by yellow arrowhead). (*B*) The fold increase in mitotic or postmitotic cells in the myr-aPKCζ-expressing sides (the number on the contralateral control side is expressed as one) are quantitatively represented. (*D–H*) Merged image from serial sections stained with Islet1 (D2 interneurons and motor neurons), 4F2 (Lim1/Lhx1 and anti-Lim2 interneurons), and mnr2/Hb9 (motor neurons) (*D*) and Tuj1 staining (*H*). (*E–G*) Abnormal localization of Pax6$^+$, Pax7$^+$, and Sox2$^+$ progenitors is indicated by yellow arrowheads. An arbitrary rectangular area free of differentiation marker in the contralateral side and, by extrapolation, an area of the same dimensions in the ipsilateral side was defined as VZ in *C*, *D*, and *H*. Similarly, an area enclosing regionalized progenitor markers was termed VZ in *E–G*. The area outside the VZ was designated MZ.

polarity results in abnormal delamination of progenitors when the aPKCζ compartmentalization is disrupted.

Mislocalization of aPKCζ Increases Progenitor Numbers and Disrupts Medial–Lateral Cell Stratification. Inheritance of the apical membrane and its constituents, such as adherens junctions, have been postulated as putative determinants of proliferative versus neurogenic divisions (1). Therefore, we assessed the consequences of the loss of apical aPKCζ compartmentalization and adherens junction compartmentalization on cell division and cell fate specification. Immunohistochemical analysis with mitosis-specific, phosphohistone H3 Serine 10 (pH3Ser10) antibody revealed that the interkinetic positions of the mitotic nuclei shifted basally from their normal location adjacent to the lumen. Thus, aPKCζ regulates the localization of mitotic progenitors at VZ (SI Fig. 6 *B* and *C*). Interestingly, there was a 2.44 ± 0.50-fold increase in the number of pH3Ser10$^+$ cells in the myr-aPKCζ-expressing neuroepithelia (Fig. 4 *A* and *B*). Similar results were obtained by staining with the mitotic marker, MPM2 (SI Fig. 6*D*). In contrast, expression of WT-aPKCζ did not affect progenitor numbers (SI Fig. 6 *E* and *F*).

Surprisingly, immunostaining for the postmitotic neuronal marker, NeuN, showed that panneuronal differentiation *per se* was unperturbed in myr-aPKCζ-expressing neural tubes (Fig. 4*C*). Analyses of overall NeuN staining intensity (as a measure of neuronal number) revealed a quantitatively similar signal on the electroporated (ipsilateral) versus the nonelectroporated control (contralateral) side (34.3 ± 5.2 to 31.7 ± 6.4 units, respectively). Concordantly, the major classes of neuronal subtypes (interneurons and motor neurons) also were specified. Similar numbers of mnr2$^+$ (69 ± 7 to 73 ± 6) and Ist1$^+$ (24 ± 5 to 19 ± 4) motor neurons were observed in the contra- and ipsilateral sides of the neural tube after myr-aPKCζ expression (n = 3) (Fig. 4*D*). Thus, despite the marked loss of cell polarity and a proper apical–basal cell axis after unlocalized aPKCζ signaling, neuronal differentiation remains relatively normal.

The primary effect of myr-aPKCζ-induced delamination was a severe disruption of the cellular stratification, leading to a mixing of distinct neural populations along the medial-lateral axis in the spinal cord. Similar to the loss of restriction of cell division within the VZ described earlier, differentiation was no longer restricted to the MZ. NeuN-expressing cells were present in the VZ (40 ± 18% differentiated neurons were mislocalized within the VZ in the electroporated side) (n = 3) (Fig. 4*C*). Similarly, interneurons and motor neurons were observed within the VZ (Fig. 4*D*). Expression of the paired box (Pax) transcription factors, Pax6 and Pax7, is normally restricted to a dorsoventral subset of medially located progenitor cells within the neural tube (17). Expression of myr-aPKCζ resulted in an increased number and the lateral dispersal of 58 ± 11% of Pax6$^+$ and 64 ± 12% Pax7$^+$ cells (n = 3) beyond the VZ (Fig. 4 *E* and *F*). A similar increase in number and displacement was seen with another progenitor marker, Sox2 (Fig. 4*G*). The effects of myr-aPKCζ are mostly cell-autonomous with respect to the neural progenitors because the displaced Pax7$^+$ cells showed aPKCζ staining along the entire apical–basal axis of the cells (SI Fig. 6*G*). Despite specification of the major classes of interneurons and motor neurons, the stratification of differentiated neurons within the MZ also was disrupted. Different classes of differentiated neurons, instead of being spatially segregated, intermingled with each other (Fig. 4*D*). Because the radial glia provide the scaffold for guided lateral migration of postmitotic neurons along the medial-lateral axis and these cells lose their apical–basal polarity when aPKCζ signaling is not localized properly (see Fig. 3*H*), it is likely that non-cell-autonomous effects on radial migration of neuronal precursors also contribute to the disruption of neuroepithelial organization. Taken together with the pattern of Tuj1 staining for neuronal-specific βIII tubulin (Fig. 4*H*), these results demonstrate that the progenitor and postmitotic populations within the spinal cord were spatially intermixed. Despite the loss of medial-lateral stratification, Pax6 and Pax7 expression remained unaltered along the dorsoventral axis. The expression of these transcription factors is precisely tuned to inductive signaling from sonic hedgehog and TGFβ factors distributed along the dorsoventral axis of the neural tube (18). Thus, neural tube patterning occurs independently of localized aPKCζ signaling.

PI3K and Rac/Cdc42 Signaling May Play an Important Role in aPKCζ-Mediated Regulation of Delamination. The activators and substrates of aPKCζ in neural progenitors remain unknown. We expressed various aPKCζ mutants in the chicken embryonic spinal cord and monitored the delamination of Pax7$^+$ cells as a sensitive bioassay for this kinase's activity. The kinase-inactive form of myr-aPKCζ (myr-aPKCζ K281W) failed to induce abnormal delamination, whereas expression of a nonmembrane-targeted aPKCζ construct that also was constitutively active because of a mutation in the pseudosubstrate domain (aPKCζ A119D) did not exhibit the strong, abnormal phenotype observed with myr-aPKCζ (Table 1). Coexpression of a kinase-dead aPKCζ (aPKCζ K281W) plus Par6A also failed to induce delamination defects (Table 1). We observed that a myristoylated form of the catalytic C-terminal kinase domain (amino acids 246–623) of aPKCζ alone was sufficient to induce abnormal delamination, albeit more weakly than full-length myr-aPKCζ (21 ± 9% regionalized progenitors found outside the VZ) (Table 1 and SI Fig. 5*B*). Thus, both membrane localization and kinase activity are obligatory features for aPKCζ function in neuroepithelial tissue organization. Our results are consistent with a recent

report that a membrane-targeted and active CAAX-DaPKC functions significantly better than a constitutively active, but predominantly cytoplasmic, ΔN-terminal DaPKC in enhancing *Drosophila* neuroblast self-renewal (19). The substitution of two conserved aspartate residues 62 and 66 within the OPR/PB1 domain of aPKCζ abolishes the aPKCζ–Par6 interaction (20). We mutated aspartates 62 and 66 in myr-aPKCζ to alanine (myr-aPKCζ D62, 66A), and expression of this mutant gave phenotypes similar to myr-aPKCζ (Table 1 and SI Fig. 5*C*). However, aPKCζ D62, 66A failed to induce delamination when coexpressed with Par6A (Table 1), indicating that the aPKCζ–Par6 complex is required when WT aPKCζ, but not when myr-aPKCζ, is expressed. The interaction of aPKCζ with Par6A is probably essential for membrane recruitment of aPKCζ, but is redundant for aPKCζ function once it is membrane-localized. In control experiments, myr-PKCε did not induce delamination defects.

The PDZ domain of Par6 inhibits aPKCζ/λ activation, but interaction with Rac/Cdc42-GTP through the CRIB domain of Par6 relieves this suppression allosterically and activates aPKCζ/λ. Moreover, it has been shown that aPKCζ functions downstream of the PI3K–PDK-1 cascade, and the phosphorylation of threonine 410 by PDK-1 has been reported to be critical for aPKCζ kinase activity in biochemical assays (21). Reports from cell culture model systems using two different neural cell types, but not neural stem cells, have previously obtained conflicting data on the requirement of PI3K and Rac/Cdc42 for aPKCζ/λ function (22, 23). To test whether Rac/Cdc42 signaling may be required for aPKCζ function in the neuroepithelium, we coexpressed WT-aPKCζ and a mutant Par6A that lacks the Rac/Cdc42-binding CRIB domain (Par6A ΔCRIB). The putative role of the PI3K signaling pathway was tested by coexpression of the PDK1 phosphorylation site mutant of aPKCζ (aPKCζ T410A), along with Par6A. In our epistasis analyses *in vivo*, both of these mutants that uncouple PI3K signaling from the Rac/Cdc42 input failed to cause abnormal delamination (Table 1), suggesting that the simultaneous activation of Rac/Cdc42 and PI3K regulates aPKCζ-dependent neural progenitors cell adhesion.

aPKCζ/λ was identified as part of a ternary complex that regulates cell adhesion in MDCK cells (10, 24), yet the effector that regulates adherens junctions downstream of aPKCζ/λ signaling remains unclear. GSK3α/β kinase is a substrate of aPKCζ and is negatively regulated by aPKCζ-dependent phosphorylation during directional astrocyte migration (23, 25) and neurite extension in hippocampal neurons (26). We explored whether phosphorylation and consequent inactivation of GSK3α/β by myr-aPKCζ also may have a role in aPKCζ-dependent regulation of adherens junctions in neural progenitors. Expression of either WT GSK3β (Table 1 and SI Fig. 5*F*) or a phosphorylation site mutant of GSK3β (GSK3β S9A) (Table 1), along with myr-aPKCζ, significantly reduced progenitor cell delamination (11 ± 7% regionalized progenitors found outside the VZ). The primary role of GSK3α/β in the canonical Wnt-signaling pathway is to phosphorylate and signal the degradation of APC and β-catenin (27). Thus, stabilized β-catenin can bind *N*-cadherin and establish adherens junctions. Moreover, by interaction with motor proteins, such as KIF3A kinesin (26, 28) and cytoplasmic dynein (23), aPKCζ and GSK3α/β also may control microtubule-dependent, polarized sorting of proteins such as *N*-cadherin to promote adherens junction assembly (29). Our data also support the notion that GSK3α/β-independent interactions of aPKCζ/λ-Par6 with polarity complexes and microtubule-binding proteins, including mLgl, Dlg, and APC (13, 30) or through the Smurf1-RhoA pathway (31), may independently contribute to delamination from the VZ. In conclusion, the localized apical activation of aPKCζ in response to Rac/Cdc42 and PI3K signaling, and the consequent spatially restricted, negative regulation of GSK3α/β, is likely to be the primary regulator of adherens junctions assembly and localization in neural progenitors (SI Fig. 7*A*). In contrast, when myr-aPKCζ or aPKCζ plus Par6A were expressed, by stoichiometry alone, most of the aPKCζ activity was localized away from the apical membrane and along the entire apical–basal axis of the progenitor cells because the apical membrane constitutes only 1–2% of the total plasma membrane volume (32). This result is likely to lead to an indiscriminate down-regulation of GSK3α/β and nonspecific aPKC-dependent interactions across the entire plasma membrane, allowing for the nonpolarized localization of adhesion molecules, consequent loss of apical junctions, and premature delamination of neural progenitors (SI Fig. 7*B*).

Discussion

Does asymmetric segregation of adherens junction molecules and apical–basal polarity in neural stem cells affect progenitor proliferation or neuronal specification? Although KO studies of adherens junction proteins or their regulators can be complicated if these proteins have pleiotropic functions (e.g., a KO of a protein with both cell-adhesion and transcriptional functions cannot be interpreted simply) or are required as stem cell determinants, a more direct approach would be to disrupt the compartmentalization of adherens junction proteins and their regulators. Disrupting this endogenous apical compartmentalization led to aberrant delamination of neural progenitors, suggesting that it is the apical membrane restriction of aPKCζ that drives apical adherens junction assembly in neural progenitors. This process, in turn, allows for the medial stratification of these cycling progenitors within the VZ. In fact, the phenotype of nonlocalized aPKCζ demonstrates that it is inadequate for aPKCζ/λ to be simply present in cells. Although the exact mechanism remains unclear, it is likely that regulated down-regulation of endogenous aPKCζ mRNA and protein in post-mitotic cells or alternatively redistribution of aPKCζ/λ constitutes the timing mechanism for the coordinated delamination during differentiation of neuronal precursors in normal development. Induced disruption of aPKCζ membrane localization, in contrast, led to an increase in cell divisions and progenitor numbers. This result is consistent with the observation that DaPKC regulates self-renewal of neuroblasts in *Drosophila* (19), and that loss of cell adhesion in α-*E*-catenin KOs (33) also results in increased symmetric division, but clearly differs from the loss of aPKCλ function, which appears to have no consequence on stem cell numbers at E15.5 (9). A temporal analysis in mice may be required to reveal this phenotype after loss of aPKCλ and adherens junctions. Nevertheless, neither Imai *et al.* nor our analyses revealed any change in neuronal specification (9). It is possible that adhesion junctions may not directly affect neurogenesis, but may function in contact inhibition that limits progenitor proliferation. Recent reports suggest that the membrane localization of aPKCλ/ι is altered in human ovarian cancer, as well as during ErbB2-mediated disruption of 3D acinar structures in MCF10A breast cancer models (34–36). Thus, an evolutionarily conserved, instructive role of apical localization of aPKCζ/λ in regulating adherens junctions also would be important in understanding mechanisms of cancer cell proliferation and metastasis. In fact, the neuroepithelial rosettes (SI Fig. 5 *L–P*) are reminiscent of Homer–Wright rosettes, which are characteristic of primitive neuroectodermal tumors or ependymoblastomas (37).

Although we have demonstrated the functional importance of subcellular localization of this kinase in progenitor proliferation and laminar organization of neural layers in the embryonic spinal cord, it remains to be investigated whether the cell biology of aPKCζ/λ localization plays a role in determining the intrinsically different neurogenic potential at different times and in different parts of the developing CNS (38). This possibility is

rather intriguing because progenitor proliferation also is observed in the subgranular zones of the dentate gyrus and the SVZ of the olfactory lobe in the adult CNS (39). In nonneural cell types, loss of compartmentalization of aPKCζ/λ exclusively at the apical membrane correlates with increased expression of Cyclin E and cell proliferation (34). Therefore, subcellular compartmentalization and the signaling pathways that regulate aPKCζ/λ activation can be of potential importance in the therapeutic regulation of neural stem cell proliferation.

Methods

Microinjection and Electroporation. Microinjection and electroporation were performed at E2, corresponding to HH stages 12–14, when the neural tube is composed mostly of neural progenitors, as described in detail in *SI Methods*. Embryos were killed on E3, E4, or E5 (HH stages 20–26), fixed, and serial sections at the level of the spinal cord were examined by immunohistochemical analyses. The constructs were expressed only in the right half of the spinal cord as a consequence of electroporation and the contralateral side serves as the endogenous control.

Immunohistochemistry. Embryos were fixed in 4% paraformaldehyde in PBS, and 10- to 14-μm frozen sections were processed for immunohistochemistry as described in *SI Methods*. After extensive washes, sections were mounted by using Gel/Mount (Biomeda) and imaged by using a Zeiss LSM 5 PASCAL laser confocal microscope. For whole-mount analyses, dsRED-expressing spinal cords were dissected and imaged by using a Zeiss Axioplan II microscope and a Princeton Instrument MicroMax-cooled CCD camera.

For quantitation of progenitor and postmitotic populations, the mitotic index was calculated by counting pH3Ser-10$^+$ or MPM2$^+$ cells. Postmitotic cell numbers were calculated by either counting NeuN$^+$ cells or, alternatively, as total fluorescence intensity (luminosity) of the MZ, which was analyzed by using the histogram function of Adobe Photoshop and expressed in arbitrary units. Results are representative of three independent experiments. Markers discussed in the text were used for quantitation of differentiated neurons within VZ and MZ.

ACKNOWLEDGMENTS. We thank Tom Jessell (Columbia University, New York), Yoshio Wakamatsu (Tohoku University, Sendai, Japan), G. Steve Martin (University of California, Berkeley, CA), Keyong Du (Tufts University School of Medicine, Medford/Somerville, MA), Alex Toker (Harvard Medical School, Boston), R. V. Farese (University of South Florida School of Medicine, Tampa, FL), Alexandra Newton (University of California at San Diego, La Jolla, CA), and the Developmental Studies Hybridoma Bank (developed under the auspices of the National Institute of Child Health and Human Development and maintained by the University of Iowa, Department of Biological Sciences) for antibodies and cDNAs; and Greg Lemke and Carla V. Rothlin for comments and suggestions during preparation of this manuscript. This work was supported by National Institutes of Health Grant CA82683, Jane Coffin Childs Fellowship for Cancer Research Project 61-1210, a Leukemia and Lymphoma Society Special Fellowship, Damon Runyon Cancer Research Association Grant DRG-1743-02, a Project Amyotrophic Lateral Sclerosis grant, and a National Institute of Neurological Disorders and Stroke grant.

1. Gotz M, Huttner WB (2005) *Nat Rev Mol Cell Biol* 6:777–788.
2. Chenn A, Zhang YA, Chang BT, McConnell SK (1998) *Mol Cell Neurosci* 11:183–193.
3. Huttner WB, Brand M (1997) *Curr Opin Neurobiol* 7:29–39.
4. Wodarz A, Huttner WB (2003) *Mech Dev* 120:1297–1309.
5. Doe CQ (2001) *Nat Cell Biol* 3:E7–E9.
6. Wodarz A, Ramrath A, Grimm A, Knust E (2000) *J Cell Biol* 150:1361–1374.
7. Rolls MM, Albertson R, Shih HP, Lee CY, Doe CQ (2003) *J Cell Biol* 163:1089–1098.
8. Horne-Badovinac S, Lin D, Waldron S, Schwarz M, Mbamalu G, Pawson T, Jan Y, Stainier DY, Abdelilah-Seyfried S (2001) *Curr Biol* 11:1492–1502.
9. Imai F, Hirai S, Akimoto K, Koyama H, Miyata T, Ogawa M, Noguchi S, Sasaoka T, Noda T, Ohno S (2006) *Development* 133:1735–1744.
10. Suzuki A, Yamanaka T, Hirose T, Manabe N, Mizuno K, Shimizu M, Akimoto K, Izumi Y, Ohnishi T, Ohno S (2001) *J Cell Biol* 152:1183–1196.
11. Manabe N, Hirai S, Imai F, Nakanishi H, Takai Y, Ohno S (2002) *Dev Dyn* 225:61–69.
12. Delalle I, Takahashi T, Nowakowski RS, Tsai LH, Caviness VS, Jr (1999) *Cereb Cortex* 9:824–832.
13. Henrique D, Schweisguth F (2003) *Curr Opin Genet Dev* 13:341–350.
14. Cole GJ, Lee JA (1997) *Brain Res Dev Brain Res* 101:225–238.
15. Ganzler-Odenthal SI, Redies C (1998) *J Neurosci* 18:5415–5425.
16. Wakamatsu Y, Maynard TM, Jones SU, Weston JA (1999) *Neuron* 23:71–81.
17. Kawakami A, Kimura-Kawakami M, Nomura T, Fujisawa H (1997) *Mech Dev* 66:119–130.
18. Tanabe Y, Jessell TM (1996) *Science* 274:1115–1123.
19. Lee CY, Robinson KJ, Doe CQ (2006) *Nature* 439:594–598.
20. Gao L, Joberty G, Macara IG (2002) *Curr Biol* 12:221–225.
21. Le Good JA, Ziegler WH, Parekh DB, Alessi DR, Cohen P, Parker PJ (1998) *Science* 281:2042–2045.
22. Shi SH, Jan LY, Jan YN (2003) *Cell* 112:63–75.
23. Etienne-Manneville S, Hall A (2001) *Cell* 106:489–498.
24. Lin D, Edwards AS, Fawcett JP, Mbamalu G, Scott JD, Pawson T (2000) *Nat Cell Biol* 2:540–547.
25. Etienne-Manneville S, Hall A (2003) *Nature* 421:753–756.
26. Shi SH, Cheng T, Jan LY, Jan YN (2004) *Curr Biol* 14:2025–2032.
27. Ciani L, Salinas PC (2005) *Nat Rev Neurosci* 6:351–362.
28. Nishimura T, Kato K, Yamaguchi T, Fukata Y, Ohno S, Kaibuchi K (2004) *Nat Cell Biol* 6:328–334.
29. Teng J, Rai T, Tanaka Y, Takei Y, Nakata T, Hirasawa M, Kulkarni AB, Hirokawa N (2005) *Nat Cell Biol* 7:474–482.
30. Etienne-Manneville S, Manneville JB, Nicholls S, Ferenczi MA, Hall A (2005) *J Cell Biol* 170:895–901.
31. Wang HR, Zhang Y, Ozdamar B, Ogunjimi AA, Alexandrova E, Thomsen GH, Wrana JL (2003) *Science* 302:1775–1779.
32. Kosodo Y, Roper K, Haubensak W, Marzesco AM, Corbeil D, Huttner WB (2004) *EMBO J* 23:2314–2324.
33. Lien WH, Klezovitch O, Fernandez TE, Delrow J, Vasioukhin V (2006) *Science* 311:1609–1612.
34. Eder AM, Sui X, Rosen DG, Nolden LK, Cheng KW, Lahad JP, Kango-Singh M, Lu KH, Warneke CL, Atkinson EN, *et al.* (2005) *Proc Natl Acad Sci USA* 102:12519–12524.
35. Zhang L, Huang J, Yang N, Liang S, Barchetti A, Giannakakis A, Cadungog MG, O'Brien-Jenkins A, Massobrio M, Roby KF, *et al.* (2006) *Cancer Res* 66:4627–4635.
36. Aranda V, Haire T, Nolan ME, Calarco JP, Rosenberg AZ, Fawcett JP, Pawson T, Muthuswamy SK (2006) *Nat Cell Biol* 8:1235–1245.
37. Harper PG, Pringle J, Souhami RL (1981) *Cancer* 48:2282–2287.
38. Caviness VS, Jr, Takahashi T, Nowakowski RS (1995) *Trends Neurosci* 18:379–383.
39. Gage FH (2000) *Science* 287:1433–1438.